

Broad-scale predictability of carbohydrates and exopolymers in Antarctic and Arctic sea ice

Graham J. C. Underwood^{a,1,2}, Shazia N. Aslam^{a,1}, Christine Michel^b, Andrea Niemi^b, Louiza Norman^c, Klaus M. Meiners^{d,e}, Johanna Laybourn-Parry^f, Harriet Paterson^g, and David N. Thomas^{c,h,i}

^aSchool of Biological Sciences, University of Essex, Colchester, Essex CO4 3SQ, United Kingdom; ^bFreshwater Institute, Fisheries and Oceans Canada, Winnipeg, MB, Canada R3T 2N6; ^cSchool of Ocean Sciences, Bangor University, Menai Bridge, Anglesey LL59 5AB, United Kingdom; ^dAntarctic Climate and Ecosystems Cooperative Research Centre and ^eInstitute of Marine and Antarctic Studies, University of Tasmania, Hobart, TAS 7001, Australia; ^fAustralian Antarctic Division, Department of Sustainability, Environment, Water, Population, and Communities, Kingston, TAS 7050, Australia; ^gBristol Glaciology Centre, University of Bristol, Bristol BS8 1SS, United Kingdom; ^hMarine Research Centre, Finnish Environment Institute (SYKE), FI-00251, Helsinki, Finland; and ⁱArctic Research Centre, DK-8000 Aarhus University, Aarhus, Denmark

Edited by Jody W. Deming, University of Washington, Seattle, WA, and approved August 15, 2013 (received for review February 15, 2013)

Sea ice can contain high concentrations of dissolved organic carbon (DOC), much of which is carbohydrate-rich extracellular polymeric substances (EPS) produced by microalgae and bacteria inhabiting the ice. Here we report the concentrations of dissolved carbohydrates (dCHO) and dissolved EPS (dEPS) in relation to algal standing stock [estimated by chlorophyll (Chl) *a* concentrations] in sea ice from six locations in the Southern and Arctic Oceans. Concentrations varied substantially within and between sampling sites, reflecting local ice conditions and biological content. However, combining all data revealed robust statistical relationships between dCHO concentrations and the concentrations of different dEPS fractions, Chl *a*, and DOC. These relationships were true for whole ice cores, bottom ice (biomass rich) sections, and colder surface ice. The distribution of dEPS was strongly correlated to algal biomass, with the highest concentrations of both dEPS and non-EPS carbohydrates in the bottom horizons of the ice. Complex EPS was more prevalent in colder surface sea ice horizons. Predictive models (validated against independent data) were derived to enable the estimation of dCHO concentrations from data on ice thickness, salinity, and vertical position in core. When Chl *a* data were included a higher level of prediction was obtained. The consistent patterns reflected in these relationships provide a strong basis for including estimates of regional and seasonal carbohydrate and dEPS carbon budgets in coupled physical-biogeochemical models, across different types of sea ice from both polar regions.

algae | microbial | biogeochemistry | global relationships

Sea ice covers extensive regions of the Arctic and Southern Oceans, as well as some subpolar seas, and exhibits major annual, interannual, and long-term climate-related variability in age, thickness, and structure (1–3). Sea ice is not an inert physical barrier to air–ocean exchange (4), and both microbial activity and physico-chemical reactions within the ice contribute to regional-scale biogeochemical processes at the air–ocean surface interface (5).

Sea ice provides a range of habitats for diverse biological assemblages that are characterized by high standing stocks of microalgae and bacteria (6). These microorganisms produce large quantities of dissolved organic carbon (DOC), often in the form of carbohydrate-rich extracellular polymeric substances (EPS) (7). Microbial EPS exist in a dynamic equilibrium from dissolved polysaccharides (dEPS <0.2 μm) to complex particulate EPS that can form gels on the millimeter to centimeter scale (8). Here we focus on the biologically relevant dissolved carbohydrates (dCHO) that constitute a substantial fraction of the DOC in sea ice (9–13) (Fig. 1). dCHO are concentrated from sea ice DOC by dialysis (>8 kDa), with subsequent treatment allowing the definition of four subcomponents of the total dCHO pool: (i) dissolved uronic acids (dUA), produced by ice diatoms and ice bacteria (14–16), that confer strong cross-linkages between

polymer chains (8), forming low solubility EPS complexes within brine channels (8, 14, 17); (ii) dEPS, produced by sea ice algae (9, 12, 18, 19) and isolated from dCHO by 70% (vol/vol) alcohol precipitation; (iii) a low solubility fraction of dEPS obtained by 30% (vol/vol) alcohol precipitation, containing complex EPS molecules (dEPS_{complex}), often produced by algae with reduced biological activity or when under physiological stress (9, 13, 19); and (iv) a fraction of highly soluble carbohydrates that are not considered EPS (dCHO_{non-EPS}), do not precipitate in alcohol, and are produced by many actively growing ice algae (9, 14).

The bacteria and algae that successfully colonize sea ice habitats have mechanisms that enable them to survive temperatures less than –20 °C and salinities >100 in the sea ice brines (17, 20). However, there is increasing evidence that the processes of seawater freezing can be biologically mediated by ice-binding proteins and EPS secreted by bacteria and algae. These compounds can alter ice structure (14, 15, 21–26) and, in the case of EPS, also form physico-chemical buffers between the organisms and the surrounding brines and ice matrix (9, 14, 17).

When sea ice melts, its dissolved and particulate constituents are released into the surface waters (27, 28), contributing to the microbial dynamics in both the melting ice and melt waters (19, 29–31). Physical aggregation of EPS in seawater to form larger particles may promote the sinking of particulate organic matter from the surface waters (19, 32), or produce EPS foams that are

Significance

Many marine microalgae and bacteria secrete polysaccharide gels (exopolymers) in response to environmental stresses, such as the freezing temperatures and salt concentrations that organisms experience when in sea ice. This study of sea ice cores from both the Antarctic and Arctic identified compelling relationships between ice thickness and salinity, algal biomass, and the concentration of polysaccharides in the ice. Knowing the first three parameters, we were able to predict the polysaccharide concentrations of the ice. This predictability is the first step in estimating the importance of such secretions to the organic carbon content of the millions of square kilometers of the ice-covered Arctic and Southern Oceans.

Author contributions: G.J.C.U., C.M., A.N., K.M.M., J.L.-P., H.P., and D.N.T. designed research; S.N.A., C.M., A.N., L.N., K.M.M., H.P., and D.N.T. performed research; S.N.A. contributed new reagents/analytic tools; G.J.C.U., S.N.A., and L.N. analyzed data; and G.J.C.U., C.M., K.M.M., J.L.-P., and D.N.T. wrote the paper.

The authors declare no conflict of interest.

This article is a PNAS Direct Submission.

¹G.J.C.U. and S.N.A. contributed equally to this work.

²To whom correspondence should be addressed. E-mail: gjcu@essex.ac.uk.

This article contains supporting information online at www.pnas.org/lookup/suppl/doi:10.1073/pnas.1302870110/-DCSupplemental.

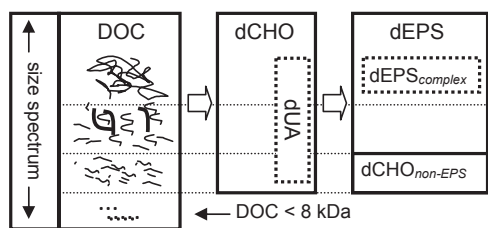


Fig. 1. Representation of the molecular-size spectrum from large polysaccharides to low molecular-weight components of the total DOC pool (<math><0.2 \mu\text{m}</math>) in melted sea ice, and partitioning of DOC into dCHO, dUA (by dialysis >8 kDa), dEPS, complex dEPS, and non-EPS carbohydrate fractions (by alcohol precipitation). Dotted boxes indicate a subcomponent of the main category.

a source of aerosol particles, which are thought to have an active role in atmospheric nucleation processes in the Arctic (33).

The growing evidence of the important role played by microbial EPS in sea ice, coupled with the changes in the extent and duration of ice cover in the polar seas (3), makes obtaining a quantitative understanding of EPS in sea ice important. Here we present a synthesis of data on dCHO—and its constituents—from sea ice samples from the Arctic and Southern Oceans, covering different seasons and variable microbial standing stocks. Our aim was to identify trends in the relationships between components of dEPS and fundamental parameters, such as temperature, ice thickness, and algal standing stock in sea ice. Using this dataset we present predictive models that can allow the estimation of dCHO and dEPS in sea ice and the potential mass of these carbon-rich organic substances on regional scales.

Results

Concentrations of Carbohydrate and dEPS in Polar Sea Ice. We analyzed 233 individual samples, obtained from 62 separate ice cores obtained from six field campaigns. These samples covered a range of ice types (first-year, multiyear, landfast, and pack ice), ice thickness, salinity, and seasonal periods (collectively the “polar” dataset) (Table S1). For the Antarctic, the winter-spring transition was covered by the SIPEX (Sea Ice Physics and Ecosystem Experiment), WWOS (Winter Weddell Outflow Study), and Prydz (Prydz Bay) datasets and the summer by the ISPOL (Ice Station Polarstern) study. For the Arctic, two spring periods were covered by the Resolute 2010 and 2011 (RES10 and RES11, respectively) data.

Concentrations of dCHO, dUA, dEPS, and dCHO_{non-EPS} ranged from 0.1 to 1,000 $\mu\text{mol C L}^{-1}$ of melted ice, and showed similar patterns across the six datasets (Fig. 2 A–D). Highest concentrations were measured in the Prydz Bay and Resolute 2010 and 2011 campaigns. Mean dCHO concentrations were similar in Antarctic ISPOL and WWOS and Arctic Resolute 2010 ice (Fig. 2A). SIPEX ice had significantly lower dUA concentrations than Prydz and Resolute 2010 and 2011 ice (Fig. 2B). dEPS varied between 5 and 500 $\mu\text{mol C L}^{-1}$, with significantly lower mean values in SIPEX and higher concentrations in Prydz, Resolute 2010, and Resolute 2011 ice (Fig. 2C). dCHO_{non-EPS} exhibited the greatest variability of all of the carbohydrate fractions (Fig. 2D), with significantly lower concentrations in Weddell Sea ice (ISPOL and WWOS) than at the other locations (Fig. 2D).

Variability between samples (within and between cores) accounted for >60% of the variance in carbohydrate concentration, with 11–28% attributed to campaign or location (Table S2). Normalization of dCHO concentrations to seawater salinity [to estimate the degree of cryo-concentration of material, or losses during brine drainage (25, 34)] revealed significant enhancement (Fig. S1) relative to average seawater concentrations

(20 $\mu\text{mol C L}^{-1}$ at all locations). There were no significant differences in mean salinity-normalized dCHO between Antarctic and mid and upper ice sections of Arctic sea ice. Bottom horizons of the Arctic ice cores (RES10b, RES11b in Fig. S1) had significantly higher mean dCHO concentrations.

Ice core chlorophyll (Chl *a*) concentration varied over six orders-of-magnitude (Fig. 2E). SIPEX ice Chl *a* concentrations were not significantly different from under-ice seawater Chl *a* concentrations (0.2 $\mu\text{g L}^{-1}$, mean of all data), but there was evidence of significant new in situ production of Chl *a* at all of the other locations. Eighty percent of the variance in Chl *a* data was a result of differences between campaigns rather than intercore or intersample variability (Table S2). DOC concentrations spanned three orders-of-magnitude, with significantly lower mean values in offshore Antarctic pack ice compared with fast ice (Prydz) and Arctic sea ice (Fig. 2F). Overall, dCHO constituted $36.4\% \pm 2.3$ (SE) of the sea ice DOC concentration (median 21%).

Correlations Between Ice Core Carbohydrate Constituents in the Polar Data.

Concentrations of Chl *a*, DOC, dUA, dCHO, dEPS, and dCHO_{non-EPS} were all significantly positively correlated (Table S3). Significant positive partial correlations demonstrated underlying relationships, independent of the high covariance in the various biomass-related measures [i.e., dCHO is a component of DOC, and algae (Chl *a*) are the main producers of DOC]. Concentrations of dEPS and dCHO_{non-EPS} were partially correlated to dCHO (Table S3), but not to each other. Although

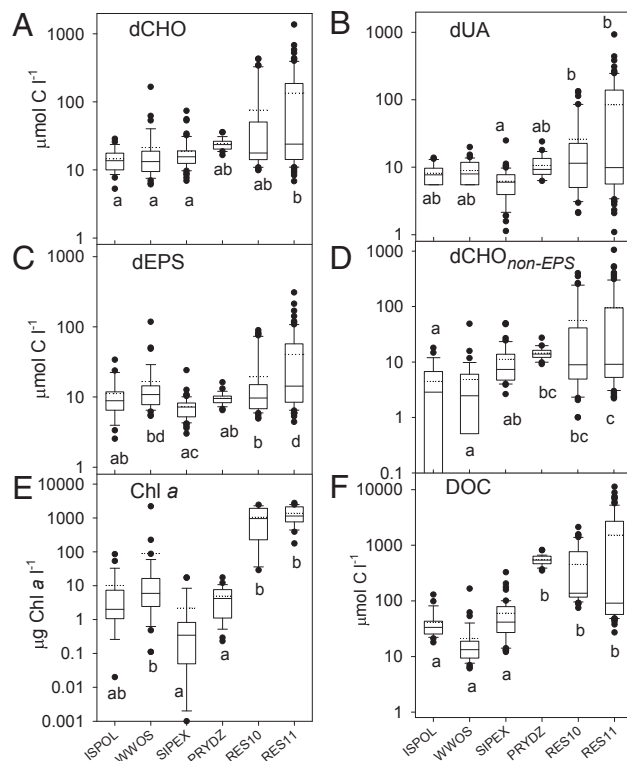


Fig. 2. Concentrations of (A) dCHO, (B) dUA, (C) dEPS, and (D) dCHO_{non-EPS}, (E) Chl *a*, and (F) DOC in melted sea ice cores from four Antarctic (ISPOL, WWOS, SIPEX, PRYDZ) and two Arctic (RES10, RES11) datasets obtained between 2004 and 2011. Box plots [median, 25th and 75th (box), 10th and 90th (error bars) percentiles, and outliers] and mean value (dotted line). Significant differences between mean values (nested GLM, $P < 0.001$) indicated by different letter codes (a, b, c; no significant differences between data with same letter code).

concentrations of dEPS followed the trend of other biomass variables, the relative proportion of dCHO consisting of complex EPS ($\%dEPS_{complex}$) was negatively correlated with dCHO ($r = -0.454$, $P < 0.01$), and positively partially correlated with increasing brine channel salinity when controlling for the relative position in ice core profile. A strong negative partial correlation, removing the influence of dCHO, between $\%dEPS_{complex}$ and the proportion of non-EPS carbohydrate ($\%dCHO_{non-EPS}$) in both the upper 90% and bottom 10% of the data subsets, indicated that ice was either relatively rich in $dEPS_{complex}$ or in $dCHO_{non-EPS}$.

Generic Sea Ice Carbohydrate Descriptive Relationships. There were significant linear relationships between dCHO and dUA, dEPS, and Chl *a* concentrations and the $\%dEPS_{complex}$ and $\%dCHO_{non-EPS}$ (Fig. 3) in the combined polar dataset. Regressions derived from concentration data (Fig. 3 A, B, and E) had significant positive slopes (Table S4). The relationship between dCHO and the proportion of the most soluble fraction ($\%dCHO_{non-EPS}$) (Fig. 3C) and with $\%dEPS_{complex}$ were opposite, with high $\%dCHO_{non-EPS}$ at high dCHO concentrations, and an increase in the relative importance of the $dEPS_{complex}$ in ice with lower overall dCHO concentrations (Fig. 3D).

The subset of data representing the bottom 10% of the core profiles (containing the majority of the algal biomass) had identical regression gradients (and higher R^2 values) to the polar dataset (Table S4). These bottom 10% relationships were based on dCHO concentration data from across the full range of available data (Fig. S2 B, D, F, H, and J), whereas the “top 90%” (colder ice) subset had a reduced data range (Fig. S2 A, C, E, G, and I) because of lower biomass present in the upper ice core horizons. Despite these differences in data range, the polar, top 90%, and bottom datasets all showed the same relationships between dCHO and dEPS (Fig. 2A, Fig. S2 E and F, and Table S3). The opposite relationships between dCHO vs. $\%dEPS_{complex}$ and dCHO vs. $\%dCHO_{non-EPS}$ were stronger (steeper slopes) in the top 90% of ice core sections (Table S4). In upper ice sections, the maximum $\%dEPS_{complex}$ was 0.66 (Table S4). In the top 90% subset, there was only a weak (although statistically significant) positive relationship between Chl *a* and dCHO (Fig. S24 and Table S3), that differed significantly from the polar data and bottom-ice regressions (Table S4).

Regression analyses for each individual campaign dataset were compared with the regression outcomes of the polar dataset. ISPOL data had no significant regression slopes, although both dEPS and $\%dCHO_{non-EPS}$ vs. dCHO had slopes similar to the polar model (Table S4). However, the majority of ISPOL data did fall within the confidence limits of the polar regressions (Fig. 2). WWOS data had significant regressions agreeing with one or more of the polar, top 90%, or bottom 10% models, except for $\%dCHO_{non-EPS}$ vs. dCHO. A similar set of regression outcomes was derived from the SIPEX data (Table S4). Sea ice from Prydz Bay (autumn-winter-spring transition) had a significant regression between dEPS vs. dCHO that matched the polar model. The Resolute 2010 and 2011 data generated site-specific regressions very similar to the global and bottom 10% models for all comparisons. Many of the regressions derived from the Arctic Resolute data were the same as those obtained from the Antarctic SIPEX and WWOS datasets (Table S4). Full details of all significant regressions are provided in Table S5.

Predictive Models for Sea Ice dCHO Concentration. Mathematical models to predict dCHO concentration were derived by a combination of best-subset analysis and least-squares approach. The best model (defined by Akaike Information Criterion (AIC)) using only physical sea ice properties to predict dCHO concentrations was based on core length, relative position in core, and ice salinity data (Fig. 4A and Table S6) ($R^2 = 46.3\%$). When Chl *a* concentration data were included, the best model was derived

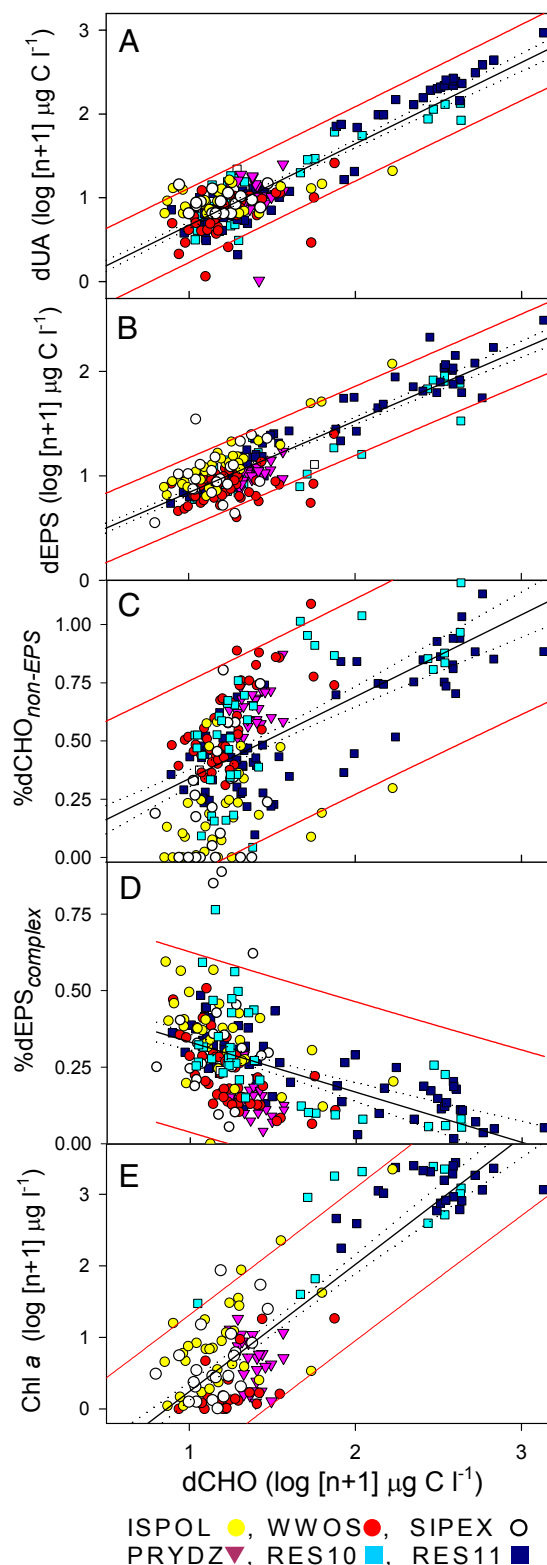


Fig. 3. Relationship between concentrations ($\mu\text{mol C L}^{-1}$) of dCHO and (A) dUA, (B) dEPS, (C) the percent contribution of non-EPS carbohydrates to overall dCHO ($\%dCHO_{non-EPS}$), (D) the percent contribution of complex EPS ($\%dEPS_{complex}$), and (E) Chl *a*, in melted ice cores from four Antarctic (ISPOL, WWOS, SIPEX, PRYDZ) and two Arctic (RES10, RES11) datasets obtained between 2004 and 2011. Concentration data are $\log(n+1)$ -transformed and percent data arcsin-transformed. Best-fit linear regression line (solid), error (dotted), and 95% confidence limits of regression (red lines) are shown for each relationship; regression details are in Table S4.

from Chl *a*, ice salinity, and core length (Fig. 4B and Table S6) ($R^2 = 77.5\%$). These “physical” and “physico-biomass” models were validated using independent data from two Southern Ocean studies, the ANT14/3 Weddell Sea summer cruise 1997 (12) (eight samples) and the ARISE austral spring cruises in 2003 (35) (16 samples). The predicted and actual carbohydrate values for these validation data fell within the 95% confidence limits of both models (Fig. 4), with levels of variability comparable to the polar datasets used in this study.

Discussion

We have shown that there are clear underlying relationships between carbohydrate and uronic acid concentrations, algal biomass, and the relative distribution of dCHO_{non-EPS} and dEPS. These relationships are consistent across a range of sea ice types from both the Arctic and Antarctic, despite differences in ice physics, chemistry, and biological activity. Concentrations of DOC and dCHO in ice are the result of a wide range of processes: incorporation of seawater DOC, cryo-concentration solubility shifts (25, 36), entrapment (17, 23) and losses as a result of brine drainage (16, 17, 23) during ice formation, in situ production by sympagic algae and bacteria (9, 11), and heterotrophic utilization (20, 30, 37). The relative importance of these factors varies over the cycle of ice formation, growth, and spring melt. Because our polar dataset covered both a wide geographical area and many seasons (Table S1), it incorporated much of this sample-specific variability, small-scale spatial heterogeneity, and temporal variation that occur within ice and

throughout the growth season (9, 19). The presence of consistent relationships across these scales of variability indicates the fundamental nature of these patterns that can be applied more generally, especially to first-year sea ice.

All datasets had the highest concentrations of carbohydrate fractions and biomass in bottom layers, decreasing in upper ice layers. Generally, concentrations were lower in Antarctic sea ice, but the lowest mean and median values were recorded in both Antarctic (ISPOL, WWOS, SIPEX) and Arctic (Resolute 2010) data. Ice sampled during the austral winter (some of SIPEX and Prydz) and some multiyear ice (ISPOL) had the lowest levels of biological activity, low Chl *a*, and some of the weakest relationships. Despite differences in ice history or properties, all of the data fit within the overall patterns and exhibited strong biological drivers, (e.g., comparison of bottom 10% and upper sections of ice cores) (Table S3). Not all of the bottom 10% sections were Chl *a* or carbohydrate-rich (Fig. S2). Upper ice was more variable, although still with significant relationships, and these colder ice samples fell within both the polar and bottom 10% prediction levels. High intersample variability in dCHO components matches previous data, demonstrating heterogeneous profiles in dCHO, DOC, texture and ice structure, and oxygen isotopic compositions down cores (37–40). This variability is a result of ice horizons in cores having formed under different growth conditions and times (41), with subsequently very different histories of “aging.” The findings contrast with the high intercampaign variability in Chl *a* concentrations, which reflects a seasonality in biomass across the six campaigns (Table S1), particularly in bottom ice layers.

High carbohydrate and EPS concentrations are associated with sea ice algal biomass and primary production (9, 12, 18, 19), as confirmed by the significant correlations (and partial correlations) in the polar dataset (Table S2). Ice algae have been estimated conservatively to contribute between 4% and 20% of total annual primary production in the ice-covered regions of the polar oceans (42) and are an important source of carbon within the ice system (42). Diatoms are a major algal group in sea ice, dominating bottom assemblages in both Arctic and Antarctic ecosystems (42, 43), and were the dominant algal group in the majority of the datasets used here (see references in Table S1). Bacteria also contribute to the EPS pool in ice (15, 20), although bacterial biomass and production is not necessarily closely coupled to algal autotrophic activity in sea ice (36). Ice diatoms and ice bacteria produce EPS with a substantial dUA content (14–16), but the relationship between dUA and dCHO was strongest in the algal-rich Resolute datasets.

The nature of EPS in sea ice transforms as the ice ages. Ice formed at the seawater interface and supporting active microbial assemblages becomes progressively cut off from underlying water as it is exposed increasingly to lower atmospheric temperatures. These changes decrease biological activity, decrease dCHO concentrations, and increase the relative importance of dEPS_{complex}, bacterial cells, and particulate EPS (9, 14, 20). The carbohydrate and EPS present in interior and upper ice horizons will have been exposed to a longer period of biological (e.g., bacterial EPS derived from heterotrophic utilization of algal DOC) and physical transformation [salinity and temperature effects (23)]. Our analyses show that the strongest relationships between the different variables investigated were present in the bottom ice sections, but that these relationships remained, albeit modified in the interior and upper, colder ice core sections. Such ice has usually lost more brine, so has a lower melted core salinity, but colder, older ice is proportionally rich in dEPS_{complex}. Such EPS can modify ice crystal formation and alter physical structure by obstructing brine drainage. These alterations could result in an aqueous environment being maintained around cells located in the high salinity environment of brine channels, facilitating microlocalization of excreted active compounds, such as ice-binding proteins (17, 22, 44).

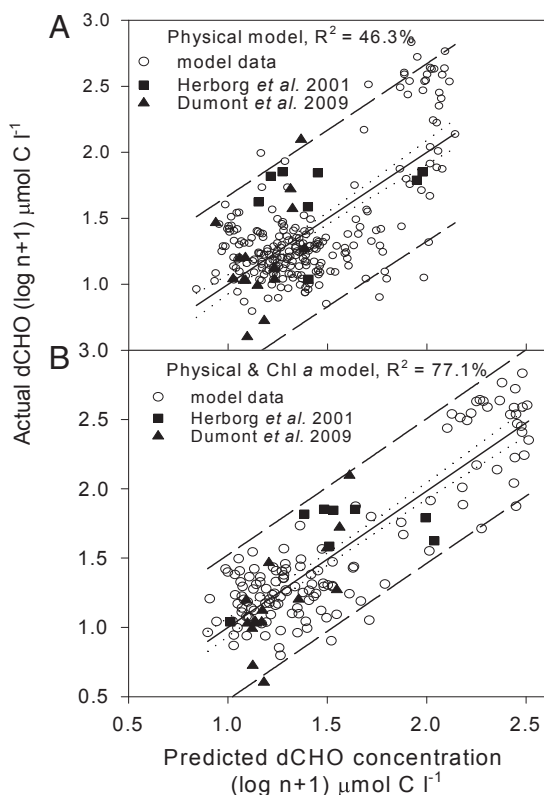


Fig. 4. Ice core carbohydrate concentrations predicted from models based on (A) ice core length, relative position in core and core salinity (physical), and (B) physical (bulk salinity, core length) and Chl *a* data, derived from a combined dataset of Antarctic and Arctic sea ice cores, compared with the measured concentrations ($\log n + 1$) of dCHO in the source ice core samples, and in two independent validation datasets (12, 35). Best-fit linear regression (solid), error (dots) and 95% confidence limits of regression (dashed) lines shown, and regression details are in Table S6.

Sea ice microbiology is influenced strongly by physical processes of sea ice formation; indeed the physical model (Fig. 4.4) predicts sea ice dCHO concentration on the basis of ice thickness, vertical position in the ice core, and core salinity. Ice thickness has been found to be key in determining sea ice Chl *a* in Antarctic pack ice (45). Approaches are being developed to assess ice thickness based on remote-sensing technologies (46, 47). Satellite data of surface temperature (2) can be used to derive temperature and salinity profiles because the temperature-depth profile is physically conserved and well matched to salinity (48), allowing the estimation of dCHO (and thus dEPS loads) within first-year sea ice. Using spatially resolved remote-sensing data would permit the application of these models to larger areal datasets and prediction of the carbon load from first-year ice to polar surface waters on ice melt. The vertical deformation and accumulation in multiyear ice (47) means that applying our models to this form of ice would not be valid. Our second model includes Chl *a*, and provides a better fit than the physical model. Airborne or satellite remote sensing cannot determine sea ice Chl *a* (because of the presence of overlying snow and ice depth), but this model could be used in association with under-ice spatial Chl *a* data, or derived from large-scale relationships between Chl *a*, ice thickness, and seasonality (45, 49).

In the Arctic, future scenarios indicate major contributions by thinner (46) first-year ice (3), which may support higher levels of biological activity than existing multiyear ice. The relationships presented here will allow the inclusion of dissolved carbohydrates and concentrations of different dEPS fractions in the developing conceptual frameworks and the modeling of sea ice carbon biogeochemistry (50) and its impacts on the underlying ocean.

Methods

Ice core samples and associated datasets were obtained as part of six separate sampling campaigns in the Antarctic and Arctic from November 2004 to May 2011 (see Table S1 for details and references to related publications). Intact ice cores, obtained using 9-cm internal diameter Kovacs MARK II corers, were sectioned in the field into 10-cm sections (bottom sections varied from 3 to 10 cm, depending on the nature of the ice), melted at <0 °C in < 24 h in the dark. The melting time varied between ice core pieces because the procedure was stopped at the point when the last ice melted in the container. Subsequently melt-water salinity was measured (ice core salinity) and subsamples were filtered through previously combusted (400 °C for 4 h) GF/F filters before freezing at -20 °C. The effective pore size of GF/F filters decreases to 0.2 μm with the precombustion process reducing the particle cutoff size to 0.2 μm, thus making filters suitable for measurement of dissolved parameters (51, 52).

Dialysis, concentration, and selective extraction procedures were used to determine the concentration of dCHO, dUA, dEPS, and non-EPS carbohydrates (9, 14, 16). Melted ice samples were dialyzed at room temperature for 8–15 h, through 8-kDa dialysis tubing (VWR) against Milli-Q water to reach a final salinity <1. Desalted samples were freeze-dried and stored at -20 °C. Subsequently samples were redissolved in 4 mL Milli-Q water (into four 1-mL aliquots). One aliquot was used for carbohydrate analysis [the term dCHO therefore describes total dissolved carbohydrate (>8 kDa) concentration]. dUA concentration in one aliquot was determined by a carbazole assay (16). Two aliquots were used for ethanol precipitation of dissolved EPS carbohydrate using either 70% (dEPS) or 30% (vol/vol) ethanol (dEPS_{complex}) overnight at 4 °C to isolate EPS components of different solubility. The dEPS_{complex} fraction contains low-solubility complex polysaccharides (16). The precipitates from each fraction were recovered by centrifugation (3,500 × g, 15 min), air-dried, and redissolved in Milli-Q water (0.65 mL). Carbohydrate concentrations in dCHO, dEPS, and dEPS_{complex} fractions were determined by a modified phenol-sulphuric acid method (9). Given known concentrations of dCHO and dEPS in each sample, the concentration of non-EPS carbohydrate [i.e., material not precipitating in 70% (vol/vol) ethanol] was calculated (CHO_{non-EPS} = dCHO - dEPS), and the percentage contributions of the two subcomponents (%dEPS_{complex} and %CHO_{non-EPS}) to the overall dCHO carbohydrate concentrations were calculated (9).

The final dataset was derived after a quality audit, removing samples with incomplete datasets (as a result of losses during processing, inadequate sample volumes to enable a full suite of measurements). A number of field

cores had complete profiles for carbohydrate concentration data but lacked Chl *a* data for some of the GF/F filters obtained during the field processing. Chl *a* determinations were conducted on adjacent cores during the Resolute 2010 campaign, and no Chl *a* measurements were made in the upper and mid section of the Resolute 2011 campaign. All these samples were retained in the dataset. Overall, this process resulted in 233 ice core sections from 62 separate ice cores (with 136 ice core sections having associated Chl *a* data) being used in the subsequent analyses (Table S1).

All concentration data deviated from normality (assessed using Bartlett's test), with high skewness caused by abundant low values. A log₁₀ (*n* + 1) transformation was used for concentration data (carbohydrate concentrations, Chl *a*), temperature, and salinity, and arcsin transformation for all proportion data (%dEPS_{complex} and %dCHO_{non-EPS}, relative position in ice core profile). The polar dataset was also divided into two subsets based on whether samples were obtained from the top 90% or the bottom 10% of any particular ice core profile, on the basis of the relative position information. Differences in sampling strategies between field campaigns resulted in an unbalanced dataset. As some samples were from adjacent positions within particular cores, we tested for spatial independence of data from samples taken within individual cores in the complete polar dataset, the polar dataset partitioned into top 90% and bottom 10% of ice core profiles, and in each campaign dataset, to determine if "core" is a significant factor. Using a nested generalized linear model (GLM) design, we determined the distribution of variance between campaign/location, core and sample on the transformed data. There were no significant "core" effects in the polar, bottom 10%, and five of the six campaign datasets, so we treated these samples as spatially independent (Table S2).

Pearson's correlation coefficients were determined on the polar and upper 90% and bottom 10% ice core-transformed datasets. To reduce the likelihood of type I errors, Bonferroni corrections of $p(\alpha)/10$ were used (a reported significance level of $P < 0.05$ required an *r* value significant at $P < 0.005$). Because of the high degree of covariance between some of the biological data, partial correlation analysis was conducted between three-way sets of data to control for the influence of a third covarying variable on any pairwise correlation.

Linear regression analysis using transformed data were conducted between each variable and total carbohydrate concentration to obtain the best-fit straight-line description $y = b + \alpha(x)$. Separate regressions for the polar, top 90%, bottom 10% and each sampling campaign datasets were conducted. Regression outcomes with α values significantly different from zero were considered significant (Table S4). Bonferroni correction of probability (α)/10 was applied to the top 90% and SIPEX regressions to accommodate for spatial nonindependence with core in those data. Curvi-linear regression was applied to the dCHO vs. %dEPS_{complex} and dCHO vs. %dCHO_{non-EPS} data, but did not create solutions with significantly higher *R*² values than the linear regressions reported. Full regression equations are given in Table S5. Comparison of regression slopes (α) were carried out between the polar, top 90% and bottom 10% data sets and the significant individual campaign regressions. Nonsignificant slopes were not compared. Bonferroni correction of $p(\alpha)/10$ was applied to ensure a conservative approach to determining differences.

Multiple linear regression was used to generate descriptive models of the relationship between ice core dCHO concentration and the physical environment descriptors (core length, salinity, temperature, relative position in core) and also with the addition of Chl *a*. A best-subset analysis approach was used, trying a number of combinations of variables. The individual multiple regressions selected by the best subset approach, were subjected to a least sum of squares approach (50) to establish most likely models. For each of these models, AIC was calculated to determine the best model, based on the lowest AIC score (53).

ACKNOWLEDGMENTS. We thank T. Cresswell-Maynard (Essex), D. Lannuzel, P. van der Merwe (Sea Ice Physics and Ecosystem Experiment, SIPEX), C. Haas, G. Dieckmann, S. Papadimitriou (Ice Station Polarstern, Winter Weddell Outflow Study), and many other colleagues without whom sampling would not have been possible; two anonymous reviewers and the editor for their thoughtful comments; and A. Dumbrell for his advice on our statistical approach. This study was funded in part by Grants NE/D00681/1 and NE/E016251/1 from the United Kingdom Natural Environment Research Council (to G.J.C.U., S.N.A., L.N., and D.N.T.); a Fisheries and Oceans Canada, Natural Sciences, and Engineering Council of Canada Individual Discovery Grant (to C.M.); invaluable field and logistical support from the Polar Continental Shelf Program (Natural Resources Canada) (C.M.); and Australian Antarctic Science Project 2751 and the University of Tasmania (to J. L-P and H.P.). The SIPEX voyage was supported by the Australian Government's Cooperative Research Centres Program through the Antarctic Climate and Ecosystems Cooperative Research Centre and Australian Antarctic Science Grant 2767.

1. Boé J, Hall A, Qu X (2009) September sea-ice cover in the Arctic Ocean projected to vanish by 2100. *Nat Geosci* 2:341–343.
2. Comiso JC (2010) Variability and trends of the global sea ice cover. *Sea Ice 2nd Edition*, eds Thomas DN, Dieckmann GS (Wiley-Blackwell, Oxford, UK) pp 205–246.
3. Stroeve JC, et al. (2012) The Arctic's rapidly shrinking sea ice cover: A research synthesis. *Clim Change* 110(3–4):1005–1027.
4. Loose B, Miller LA, Elliott S, Papakyriakou T (2011) Sea ice biogeochemistry and material transport across the frozen interface. *Oceanography (Wash DC)* 24:202–218.
5. Rysgaard S, et al. (2011) Sea ice contribution to the air–sea CO₂ exchange in the Arctic and Southern Oceans. *Tellus* 63(5):823–830.
6. Thomas DN, Dieckmann GS eds (2010) *Sea Ice 2nd Edition*, (Wiley-Blackwell, Oxford, UK).
7. Thomas DN, Papadimitriou S, Michel C (2010) Biogeochemistry of sea ice. *Sea Ice 2nd Edition*, eds Thomas DN, Dieckmann GS (Wiley-Blackwell, Oxford, UK) pp 425–467.
8. Verdugo P (2012) Marine microgels. *Annu Rev Mar Sci* 4:375–400.
9. Underwood GJC, Fietz S, Papadimitriou S, Thomas DN, Dieckmann GS (2010) Distribution and composition of dissolved extracellular polymeric substances (EPS) in Arctic sea ice. *Mar Ecol Prog Ser* 404:1–19.
10. Krembs C, Eicken H, Junge K, Deming JW (2002) High concentration of exopolymeric substances in Arctic winter seawater: Implication for the polar ocean carbon cycle and cryoprotection of diatoms. *Deep Sea Res Part I Oceanogr Res Pap* 49(12):2163–2181.
11. Riedel A, Michel C, Gosselin M, LeBlanc B (2007) Enrichment of nutrients, exopolymeric substances and microorganisms in newly formed sea ice on the Mackenzie shelf. *Mar Ecol Prog Ser* 342:55–67.
12. Herborg L-M, Thomas DN, Kennedy H, Haas C, Dieckmann GS (2001) Dissolved carbohydrates in Antarctic sea ice. *Antart Sci* 13(2):119–125.
13. Norman L, et al. (2011) The characteristics of dissolved organic matter (DOM) and chromophoric dissolved organic matter (CDOM) in Antarctic sea ice. *Deep Sea Res Part II Top Stud Oceanogr* 58(9–10):1075–1091.
14. Aslam SN, Cresswell-Maynard T, Thomas DN, Underwood GJC (2012a) Production and characterization of the intra- and extracellular carbohydrates and polymeric substances (EPS) of three sea-ice diatom species, and evidence for a cryoprotective role for EPS. *J Phycol* 48(6):1494–1509.
15. Nichols CM, et al. (2005) Chemical characterization of exopolysaccharides from Arctic marine bacteria. *Microb Ecol* 49(4):578–589.
16. Aslam SN, et al. (2012b) Dissolved extracellular polymeric substance (dEPS) dynamics and bacterial growth during sea ice formation in an ice tank study. *Polar Biol* 35(5):661–676.
17. Krembs C, Eicken H, Deming JW (2011) Exopolymer alteration of physical properties of sea ice and implications for ice habitability and biogeochemistry in a warmer Arctic. *Proc Natl Acad Sci USA* 108(9):3653–3658.
18. Meiners K, Gradinger R, Fehling J, Citivarese G, Spindler M (2003) Vertical distribution of exopolymer particles in sea ice of the Fram Strait (Arctic) during Autumn. *Mar Ecol Prog Ser* 248:1–13.
19. Riedel A, Michel C, Gosselin M (2006) Seasonal study of sea-ice exopolymeric substances on the Mackenzie shelf: Implications for transport of sea-ice bacteria and algae. *Aquat Microb Ecol* 45:195–206.
20. Collins RE, Carpenter SD, Deming JW (2008) Spatial heterogeneity and temporal dynamics of particles, bacteria and pEPS in Arctic winter sea ice. *J Mar Syst* 74:902–917.
21. Junge K, Eicken H, Deming JW (2004) Bacterial Activity at –2 to –20 °C in Arctic wintertime sea ice. *Appl Environ Microbiol* 70(1):550–557.
22. Raymond JA, Janech MG, Fritsen CH (2009) Novel ice-binding proteins from a psychrophilic Antarctic alga (*Chlamydomonadaceae*, *Chlorophyceae*). *J Phycol* 45(1E):130–136.
23. Krembs C, Deming JW (2008) The role of exopolymers in microbial adaptation to sea-ice. *Psychrophiles: From Biodiversity to Biotechnology*, eds Margesin R, et al. (Springer, Berlin, Heidelberg) pp 247–264.
24. Juhl AR, Krembs C, Meiners KM (2011) Seasonal development and differential retention of ice algae and other organic fractions in first year Arctic sea ice. *Mar Ecol Prog Ser* 436:1–16.
25. Ewert M, Deming JW (2011) Selective retention in saline ice of extracellular polysaccharides produced by the cold-adapted marine bacterium *Colwellia psychrerythraea* strain 34H. *Ann Glaciol* 52(57):111–117.
26. Bayer-Giraldi M, Weikusat I, Besir H, Dieckmann G (2011) Characterization of an antifreeze protein from the polar diatom *Fragilariopsis cylindrus* and its relevance in sea ice. *Cryobiology* 63(3):210–219.
27. Petrou K, Ralph PJ (2011) Photosynthesis and net primary productivity in three Antarctic diatoms: Possible significance for their distribution in the Antarctic marine ecosystem. *Mar Ecol Prog Ser* 437:27–40.
28. Boetius A, et al.; RV Polarstern ARK27-3-Shipboard Science Party (2013) Export of algal biomass from the melting Arctic sea ice. *Science* 339(6126):1430–1432.
29. Paterson H, Laybourn-Parry J (2012) Sea ice microbial dynamics over an annual ice cycle in Prydz Bay, Antarctica. *Polar Biol* 35(7):993–1002.
30. Meiners K, Krembs C, Gradinger R (2008) Exopolymer particles: Microbial hotspots of enhanced bacterial activity in Arctic fast ice (Chukchi Sea). *Aquat Microb Ecol* 52:195–207.
31. Lannuzel D, et al. (2010) Distribution of dissolved iron in Antarctic sea ice: Spatial, seasonal, and inter-annual variability. *J Geophys Res* 115:G03022.
32. Riebesell U, Schloss I, Smetacek V (1991) Aggregation of algae released from melting sea ice: Implications for seeding and sedimentation. *Polar Biol* 11(4):239–248.
33. Leck C, Bigg EK (2010) New particle formation of marine biological origin. *Aerosol Sci Technol* 44(7):570–577.
34. Müller S, et al. (2013) Selective incorporation of dissolved organic matter (DOM) during sea ice formation. *Mar Chem* 155:148–157.
35. Dumont I, et al. (2009) Distribution and characterization of dissolved and particulate organic matter in Antarctic pack ice. *Polar Biol* 32(5):733–750.
36. Collins RE, Rocap G, Deming JW (2010) Persistence of bacterial and archaeal communities in sea ice through an Arctic winter. *Environ Microbiol* 12(7):1828–1841.
37. Meiners K, Brinkmeyer R, Granskog MA, Lindfors A (2004) Abundance, size distribution and bacterial colonisation of exopolymeric particles in Antarctic sea ice. (Bellingshausen Sea). *Aquat Microb Ecol* 35:283–296.
38. van der Merwe P, et al. (2009) Biogeochemical observations during the winter spring transition in East Antarctic sea ice: Evidence of iron and exopolysaccharide controls. *Mar Chem* 115(3–4):163–175.
39. Meiners KM, et al. (2011) Physico-ecobiogeochemistry of East Antarctic pack ice during the winter-spring transition. *Deep Sea Res Part II Top Stud Oceanogr* 58(9–10):1172–1181.
40. Riedel A, Michel C, Gosselin M, LeBlanc B (2008) Winter-spring dynamics in sea-ice carbon cycling on the Mackenzie shelf, Canadian Arctic. *J Mar Syst* 74(3–4):918–932.
41. Willmes S, Haas C, Nicolaus M (2011) High radar-backscatter regions on Antarctic sea-ice and their relation to sea-ice and snow properties and meteorological conditions. *Int J Remote Sens* 32(14):3967–3984.
42. Arrigo KR, Mock T, Lizotte MP (2010) Primary producers in sea ice. *Sea Ice 2nd Edition*, eds Thomas DN, Dieckmann GS (Wiley-Blackwell, Oxford, UK) pp 283–325.
43. Caron DA, Gast RJ (2010) Heterotrophic protists associated with sea ice. *Sea Ice 2nd Edition*, eds Thomas DN, Dieckmann GS (Wiley-Blackwell, Oxford, UK) pp 327–356.
44. Janech MG, Krell A, Mock T, Kang JS, Raymond JA (2006) Ice-binding proteins from sea ice diatoms (*Bacillariophyceae*). *J Phycol* 42(2):410–416.
45. Meiners KM, et al. (2012) Chlorophyll *a* in Antarctic sea ice from historical ice core data. *Geophys Res Lett* 39:L21602.
46. Giles KA, Laxon SW, Ridout AL (2008) Circumpolar thinning of Arctic sea ice following the 2007 record ice extent minimum. *Geophys Res Lett* 35(22):L22502.
47. Haas C (2010) Dynamics versus thermodynamics: The sea ice thickness distribution. *Sea Ice 2nd Edition*, eds Thomas DN, Dieckmann GS (Wiley-Blackwell, Oxford, UK) pp 113–152.
48. Petrich C, Eicken H (2010) Growth, structure and properties of sea ice. *Sea Ice 2nd Edition*, eds Thomas DN, Dieckmann GS (Wiley-Blackwell, Oxford, UK) pp 23–77.
49. Fritsen CH, et al. (2010) The timing of sea ice formation and exposure to photosynthetically active radiation along the Western Antarctic Peninsula. *Polar Biol* 34(5):683–692.
50. Vancoppenolle M, et al. (2013) Role of sea ice in global biogeochemical cycles: Emerging views and challenges. *Quat Sci Rev*, 10.1016/j.quascirev.2013.04.011.
51. Nayar S, Chou LM (2003) Relative efficiencies of different filters in retaining phytoplankton for pigment and productivity studies. *Estuar Coast Shelf Sci* 58(2):241–248.
52. Hulatt CJ, Thomas DN (2010) Dissolved organic matter (DOM) in microalgal photobioreactors: A potential loss in solar energy conversion? *Bioresour Technol* 101(22):8690–8697.
53. Matthiopoulos J (2011) *How to be a Quantitative Ecologist: The 'A to R' of Green Mathematics and Statistics* (John Wiley, Chichester, UK).